

# Effect of Zn doping on the microwave absorption of BFO multiferroic materials

S Bi<sup>1</sup>, J Li, B Mei, X J Su, C Z Ying and P H Li

Xi'an Research Institute of High-Tech, Xi'an, 710025, China

<sup>1</sup>E-mail: bisong5011@163.com

**Abstract.** The microwave absorbing materials were firstly used in the Second World War. And the BiFeO<sub>3</sub> (BFO) based microwave absorbers have been widely applied into the microwave absorbing area due to its possession of excellent electromagnetic properties. Various methods have been conducted to improve the microwave absorption performance of the BFO based materials. In the work, the sol-gel method were used to prepare the BFO, and the Zn were doped into the BFO to prepare the Bi<sub>1-x</sub>Zn<sub>x</sub>FeO<sub>3</sub> nanoparticles. The X-ray diffraction, scanning electron microscope, and vector network analysis (VNA) were conducted to characterize the microstructure and electromagnetic properties of the as-prepared samples. The results indicate that the Bi<sub>1-x</sub>Zn<sub>x</sub>FeO<sub>3</sub> nanoparticles were successfully gained and the as-prepared samples possess excellent microwave absorption properties.

## 1. Introduction

With the development of the electronic industry, including electronic communication and computer office, the electromagnetic pollution becomes worse and worse in our daily life. With the development of the radar technique, the demand of the microwave absorbing materials that possess excellent wave absorption performance is urgency. BiFeO<sub>3</sub> based microwave absorbing material is the traditional microwave absorber due to the long-range spiral spin modulation (period length of 64 nm), and the materials are one of most used multiferroic materials. Significant efforts have been dedicated to understanding their intrinsic properties and various methods were conducted to improve the microwave absorbing properties of the composites [1-7]. However, the macroscopic magnetization of BFO is quite small, thus greatly restricting its practical applications [8-9]. When the substitution concentration reaches a high level, the ferroelectricity is often decreased, which is originated from the space group transformation or the decrease in the stereochemical activity of Bi lone electron pairs [10-15].

Intensive research has been focused on tuning magnetization of the BFO based materials to achieve effective microwave absorption. In particular, cation doping has shown unique advantages among all the different approaches [16-21]. For example, Li et al. [22] have investigated Ca-doped BFO nanoparticles, and the qualified bandwidth in X-band was successfully increased to 3.4 GHz. Besides, in the La-substituted BFO investigated by Cao and his coworkers, the minimum reflection loss was elevated from -12 dB to -30dB [23]. In the work, we utilized the sol-gel method to prepare the Zn-doped BFO Bi<sub>1-x</sub>Zn<sub>x</sub>FeO<sub>3</sub> (x=0.1, 0.15, 0.2) samples, and the dielectric properties of the as-prepared samples are discussed.



## 2. Experimental

The sol-gel method was used to prepare the  $\text{Bi}_{1-x}\text{Zn}_x\text{FeO}_3$  ( $x=0.1, 0.15, 0.2$ ) samples, and ethylene glycol was used as the solvent. Firstly, stoichiometric amounts of  $\text{Bi}(\text{NO}_3)_3 \cdot 5\text{H}_2\text{O}$ ,  $\text{Fe}(\text{NO}_3)_3 \cdot 9\text{H}_2\text{O}$  and  $\text{Zn}(\text{NO}_3)_2 \cdot 6\text{H}_2\text{O}$  were dissolved in ethylene glycol and then mixed together, the mixture was heated to  $50^\circ\text{C}$  until the sol solution were obtained. Then the xerogel was obtained by continually stirring the solution at  $90^\circ\text{C}$ . Subsequently, the powders were put into the tube furnace to heat at  $120^\circ\text{C}$  for 1 h followed by a treatment at  $300^\circ\text{C}$  for 2 h. Then, the samples were finely ground into powders. Finally, the powders were calcined in tube furnace at  $650^\circ\text{C}$  for 1 h for cooled quickly, and the powders washed by deionized water.

## 3. Results and discussion

As is shown in figure 1, the XRD patterns of the Zn-substituted BFO ( $x=0.1, 0.15, 0.2$ ) were characterized by X-ray diffraction (XRD, Rigaku Ultima IV, Cu-K $\alpha$ ) in the range of  $15^\circ \sim 90^\circ$  with a scan speed of 3 s per step, and a step size of  $0.02^\circ$  in  $2\theta$ . Comparing the X patterns of the Zn-substituted BFO ( $x=0.1, 0.15, 0.2$ ) with the pure BFO, it is obvious that the distinct peaks around  $22^\circ$ ,  $32^\circ$ ,  $38^\circ$ ,  $46.5^\circ$  and  $53^\circ$  are all presented in the three patterns, indicating that the  $\text{Zn}^{2+}$  have replaced the  $\text{Bi}^{3+}$ . Therefore, in the work, the  $\text{Bi}_{1-x}\text{Zn}_x\text{FeO}_3$  ( $x=0.1, 0.15, 0.2$ ) nanoparticles were successfully obtained.

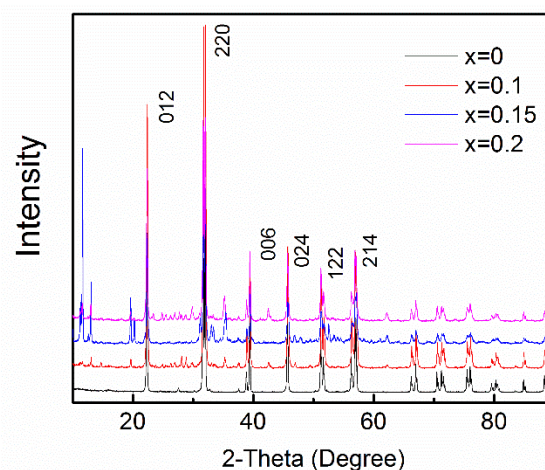


**Figure 1.** XRD patterns of the  $\text{Bi}_{1-x}\text{Zn}_x\text{FeO}_3$  ( $x=0.1, 0.15$  and  $0.2$ ) nanoparticles.

The microstructure of the as-prepared  $\text{Bi}_{1-x}\text{Zn}_x\text{FeO}_3$  ( $x=0.1, 0.15$  and  $0.2$ ) nanoparticles was demonstrated in figure 2. It is obvious that the  $\text{Bi}_{1-x}\text{Zn}_x\text{FeO}_3$  samples are well-crystallized and have uniform particle size distribution. The average particle sizes are roughly 130, 110 and 100 nm for the  $\text{Bi}_{0.9}\text{Zn}_{0.1}\text{FeO}_3$ ,  $\text{Bi}_{0.85}\text{Zn}_{0.15}\text{FeO}_3$  and  $\text{Bi}_{0.8}\text{Zn}_{0.2}\text{FeO}_3$  samples, respectively. Therefore, it can be concluded that the particle sizes do not have a significant impact on the electromagnetic performance of the samples, and the well crystallized samples were gained.

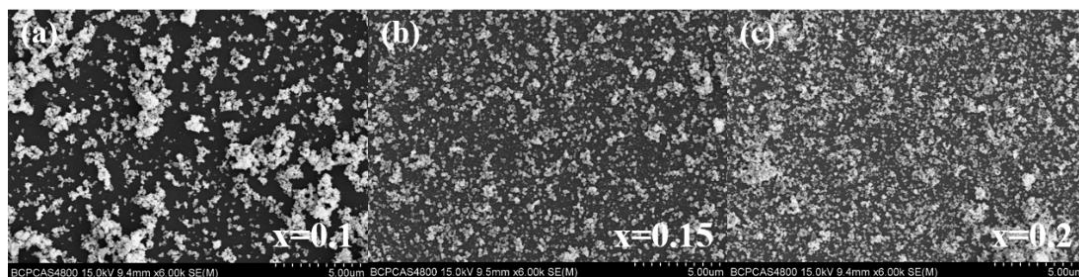


**Figure 2.** SEM images of the  $\text{Bi}_{1-x}\text{Zn}_x\text{FeO}_3$  ( $x=0.1, 0.15$  and  $0.2$ ) nanoparticles.

The vector network analyzer (VNA, E5071C KEYSIGHT) was used to characterize the permittivity and permeability of the as-prepared samples (8.2~12.4 GHz) via coaxial method. In the preparation of the samples, paraffin was used for the matrices. The inner diameter of the specimens is 3 mm, and the external diameter is 6.9 mm. The frequency-dependent complex permittivity ( $\epsilon$ ) and permeability ( $\mu$ ) of the samples are exhibited on figure 3. It is obvious that with the increase of frequency, the permittivity of the samples all have a slight decline trend. The real permittivities of the  $\text{Bi}_{0.9}\text{Zn}_{0.1}\text{FeO}_3$ ,  $\text{Bi}_{0.85}\text{Zn}_{0.15}\text{FeO}_3$  and  $\text{Bi}_{0.8}\text{Zn}_{0.2}\text{FeO}_3$  are roughly up to 10.3, 13.2 and 8.6, respectively.

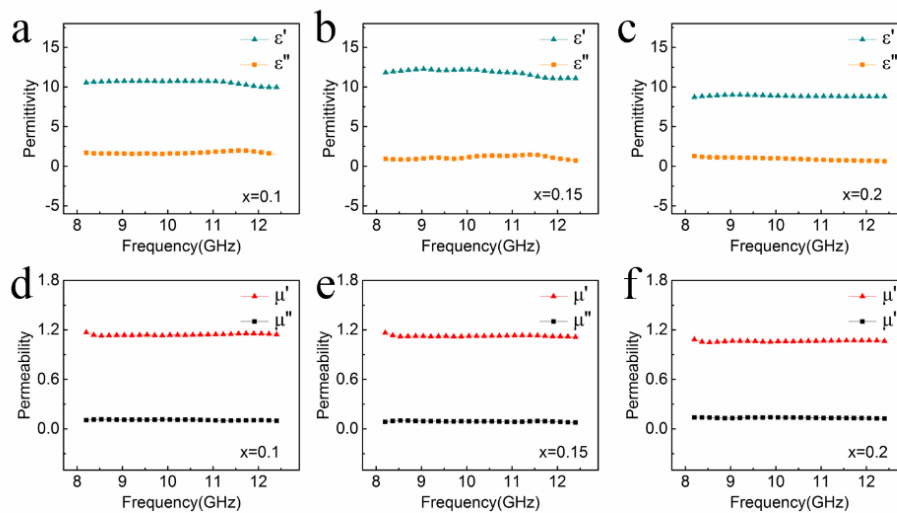


**Figure 3.** Frequency-dependent permittivity and permeability of the  $\text{Bi}_{1-x}\text{Zn}_x\text{FeO}_3$ .

The reflection loss ( $R_L$ ) is achieved by the relation:

$$R_L = 20 \log(|Z_{in} - 1| / |Z_{in} + 1|) \quad (1)$$

Here  $Z_{in}$  refers to the input impedance of the absorption layer, which could be achieved by:

$$Z_{in} = (\mu_r / \epsilon_r)^{1/2} \tanh[j2\pi f d (\mu_r \epsilon_r)^{1/2} / c] \quad (2)$$

where,  $\mu_r$  and  $\epsilon_r$  are the complex permittivity and permeability of the samples, respectively,  $f$  is frequency,  $d$  is thickness of the absorber, and  $c$  is the light velocity. Meanwhile, it could be the reflection the ability of the microwave absorption performance of the absorber,

The microwave absorption performance of the as-prepared samples at different frequency were calculated by the relation (1 and 2), and the microwave absorption performance of the as-prepared samples at different thickness (4mm, 5mm, 6mm) were shown in figure 4. Apparently, the qualified bandwidth (QB,  $RL < -10\text{dB}$ ) of the  $\text{Bi}_{0.9}\text{Zn}_{0.1}\text{FeO}_3$  nanoparticles is 0.8 GHz at the thickness of 4mm. The QB reaches 1 GHz at the thickness of 6mm, and the QB is 0.6 GHz at the thickness of 6mm. Likewise, the QB of the  $\text{Bi}_{0.85}\text{Zn}_{0.15}\text{FeO}_3$  nanoparticles is 1.1 GHz at the thickness of 5mm, and that of the  $\text{Bi}_{0.85}\text{Zn}_{0.15}\text{FeO}_3$  nanoparticles at the thickness of 6mm reaches 1.4 GHz. Besides, the QB of the  $\text{Bi}_{0.8}\text{Zn}_{0.2}\text{FeO}_3$  nanoparticles is 1.1 GHz at the thickness of 4mm. The QB is 1 GHz at the thickness of 5mm, and that of the  $\text{Bi}_{0.85}\text{Zn}_{0.15}\text{FeO}_3$  nanoparticles at the thickness of 6mm is 0.6 GHz.

According to figure 4, the minimum reflection loss ( $RL_{min}$ ) of the  $\text{Bi}_{0.9}\text{Zn}_{0.1}\text{FeO}_3$  nanoparticles reaches  $-22.12\text{dB}$ , and the  $RL_{min}$  of  $\text{Bi}_{0.8}\text{Zn}_{0.2}\text{FeO}_3$  nanoparticles is  $-18.75\text{dB}$ . And the minimum reflection loss of the  $\text{Bi}_{0.85}\text{Zn}_{0.15}\text{FeO}_3$  nanoparticles reaches  $-29.89\text{dB}$ . Consequently, it is obvious that the composites possess best microwave absorption performance when the Zn doping ratio is 15%.

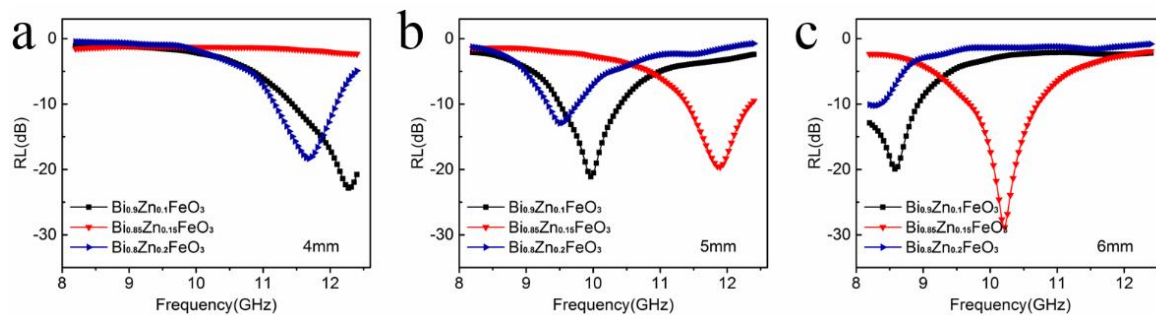


**Figure 4.** Microwave absorption performance of the as-prepared samples at different thickness.

Therefore, the as-prepared  $\text{Bi}_{1-x}\text{Zn}_x\text{FeO}_3$  nanoparticles were characterized and the microwave absorption performance of the composites were discussed. Consequently, the composites perform well in electromagnetic loss area, especially when the doping ratio is 15%. Moreover, the density of the BFO based composites is relatively low compared with the traditional absorbing materials, thus the study provides a guide for preparing microwave absorbing materials that possess excellent electromagnetic loss performance.

#### 4. Conclusion

In summary, the  $\text{Bi}_{1-x}\text{Zn}_x\text{FeO}_3$  composites are successfully prepared by sol-gel method. The microstructure and the electromagnetic properties of the as-prepared samples were characterized. The results show that the  $\text{Bi}_{1-x}\text{Zn}_x\text{FeO}_3$  samples are crystallize well, have uniform particle size distribution and have the lowest dielectric losses when the doping ratio of  $\text{Zn}^{2+}$  is 15%. The as-prepared  $\text{Bi}_{0.85}\text{Zn}_{0.15}\text{FeO}_3$  nanoparticles exhibit excellent microwave absorbing abilities at the thickness of 6mm. The qualified bandwidth of the samples is 1.4 GHz, and the minimum reflection loss of the samples reaches -29.89dB. Consequently, the study may provide a guide to explore a material that performs well in microwave absorption area.

#### References

- [1] CJ Li, B Wang, JN Wang 2012 Magnetic and Microwave Absorbing Properties of Electrospun  $\text{Ba}_{(1-x)}\text{La}_x\text{Fe}_{12}\text{O}_{19}$  Nanofibers *J. Magn. Magn. Mater.* **324** 1305-1311
- [2] ZN Yang, F Luo, Y Hu, DM Zhu, WC Zhou 2016 Dielectric and microwave absorption properties of  $\text{TiAlCo}$  ceramic fabricated by atmospheric plasma spraying *Ceram. Int.* **42** 8525-8530
- [3] YJ Kim, SS Kim 2010 Magnetic and microwave absorbing properties of Ti and Co substituted M-hexaferrites in Ka-band frequencies (26.5~40 GHz) *J. Electrochem* **24** 314-318
- [4] PJ Liu, ZJ Yao, JT Zhou 2016 Fabrication and microwave absorption of reduced graphene oxide/ $\text{Ni}_{0.4}\text{Zn}_{0.4}\text{Co}_{0.2}\text{Fe}_2\text{O}_4$  nanocomposites *Ceram. Int.* **42** 9241-9249
- [5] HS Chen, WY Wei, JX Liu, DN Fang 2012 Propagation of a mode-III interfacial crack in a piezoelectric-piezomagnetic bi-material *Int. J. Solids Struct.* **49** 2547-2558
- [6] HS Chen, J Ma, YM Pei, DN Fang 2013 Anti-plane Yoffe-type crack in ferroelectric materials *Int. J. Fract.* **179** 35-43
- [7] HS Chen, HL Wang, YM Pei, YJ Wei, B Lin, DN Fang 2015 Crack instability of ferroelectric solids under alternative electric loading *J. Mech. Phys. Solids.* **81** 75-90
- [8] L Zhou, S Cui, Y Zhai, F Luo, YY Dong 2015 Dielectric and microwave absorption properties of plasma sprayed  $\text{Cr/Al}_2\text{O}_3$  composite coatings *Ceram. Int.* **41** 14908-14914
- [9] Z Amouzegar, R Naghizadeh, HR Rezaiea, M Ghahari, M Aminzare 2015 Cubic  $\text{ZnWO}_4$  nanophotocatalysts synthesized by the microwave-assisted precipitation technique *Ceram. Int.* **41** 1743-1747
- [10] J Liu, M. Cao, Q Luo, HL Shi, WZ Wang, J Yuan 2016 Electromagnetic Property and Tunable Microwave Absorption of 3D Nets from Nickel Chains at Elevated Temperature *Acs Appl.*



*Mater. Interfaces* **8** 22615-22622

- [11] H Tang, et al 2016 Fe<sub>3</sub>C/helical carbon nanotube hybrid: Facile synthesis and spin induced enhancement in microwave absorbing properties *Compos. Part B* **107** 51-58
- [12] CS Dong, X Wang, PH Zhou, T Liu, JL Xie, LJ Deng 2014 Microwave magnetic and absorption properties of M-type ferrite BaCo<sub>x</sub>Ti<sub>x</sub>Fe<sub>12-2x</sub>O<sub>19</sub> in the Ka band *J. Magn. Magn. Mater.* **354** 340-344
- [13] YP Wang, Z Peng, W Jiang 2016 Controlled synthesis of Fe<sub>3</sub>O<sub>4</sub>@SnO<sub>2</sub>/RGO nano composite for microwave absorption enhancement *Ceram. Int.* **42** 10682-10689
- [14] HS Chen, WY Wei, JX Liu, DN Fang 2014 Propagation of a semi-infinite conducting crack in piezoelectric materials: Mode-I problem *J. Mech. Phys. Solids.* **68** 77-92
- [15] Li Yong, Cao Mao-sheng, Wang Da-wei, Yuan Jie 2015 High-efficiency and dynamic stable electromagnetic wave attenuation for La doped bismuth ferrite at elevated temperature and gigahertz frequency *RSC Adv.* **5** 77184-77191
- [16] N S Sowmya, A Srinivas, P Suresh, A Shukla and S V Kamat 2015 Synthesis and study of structural, magnetic and microwave absorption properties in multiferroic BiFeO<sub>3</sub> electroceramic *J. Mater. Sci.: Mater. Electron.* **26** 5368-5379
- [17] ZL Hou, HF Zhou, LB Kong, HB Jin, X Qi, MS Cao 2012 Enhanced ferromagnetism and microwave absorption properties of BiFeO<sub>3</sub> nanocrystals with Ho substitution *Mater. Lett.* **84** 110-113
- [18] FS Wen, N Wang, F Zhang 2010 Enhanced microwave absorption properties in BiFeO<sub>3</sub> ceramics prepared by high-pressure synthesis *Solid State Commun.* **150** 1888-1891
- [19] HJ Yang, WQ Cao, DQ Zhang, TJ Su, HL Shi, WZ Wang, J Yuan, MS Cao 2015 NiO Hierarchical Nanorings on SiC: Enhancing Relaxation to Tune Microwave Absorption at Elevated Temperatures *Acs Appl. Mater. Interfaces* **13** 70-73
- [20] E Bahraoui, M Taibi, AM ET S Tlemc, AA Albassam, MA Lefdil, IV Kityk, NS AlZayed 2015 Multiferroic Eu doped BiFeO<sub>3</sub> microparticle polymer composites as materials for laser induced gratings *Journal Materials Science: Materials in Electronics* **26** 9949-9954
- [21] CY Quan, Y Han, N Gao, WW Mao, J Zhang, JP Yang, XA Li, W Huang 2016 Comparative studies of pure, Ca-doped, Co-doped and co-doped BiFeO<sub>3</sub> nanoparticles *Ceram. Int.* **42** 537-544
- [22] ZJ Li, ZL Hou, WL Song, XD Liu, WQ Cao, XH Shao, MS Cao 2016 Unusual continuous dual absorption peaks in Ca-doped BiFeO<sub>3</sub> nanostructures for broadened microwave absorption *Nanoscale* (**19**) 10415-10424
- [23] Y Li, HJ Yang, WG Yang, ZL Hou, JB Li, HB Jin, J Yuan MS Cao 2013 Structure, ferromagnetism and microwave absorption properties of La substituted BiFeO<sub>3</sub> nanoparticles *Mater. Lett.* **111** 130-137